Allyltrimethylsilane polymers from metallocene catalysts: tacticity and structural characterization

Robert Zeigler*
Himont Research and Development Center, 912 Appleton Road, Elkton, Maryland 21921, USA

and Luigi Resconi and Giulio Balbontin
Himont Italia S.r.l., G. Natta Research Center, P. le G. Donegani 12, I-44100 Ferrara, Italy

and Gaetano Guerra*, Vincenzo Venditto and Claudio De Rosa
Dipartimento di Chimica, Università di Napoli, via Mezzocannone 4, I-80134 Napoli, Italy
(Received 18 January 1994)

The synthesis of isotactic, syndiotactic and atactic poly(allyltrimethylsilane) (PATMS) is described, along with the characterization of these polymers using thermal methods, X-ray diffraction, solution and solid-state nuclear magnetic resonance (n.m.r.). Isotactic PATMS was produced from *rac*-$Me_2SiInd_2ZrCl_2$/MAO (methylalumoxane) and displayed chains with an s(3/1) symmetry in the crystalline domains. Syndiotactic PATMS, produced from $Me_2C(Cp)(Flu)ZrCl_2$/MAO, was a semicrystalline polymer with chains in the crystalline phase exhibiting s(2/1)2 helical symmetry. A combined X-ray diffraction and solid-state n.m.r. analysis on poorly crystallized samples of syndiotactic PATMS indicates the occurrence in the crystalline phase, for given crystallization conditions, of disorder in the packing of chains, which preserve the helical conformation. Atactic PATMS, an amorphous polymer, was produced using an Ind_2ZrCl_2/MAO catalyst.

(Keywords: poly(allyltrimethylsilane); synthesis; characterization)

INTRODUCTION

As one of the vinyl monomers that undergo polymerization with Ziegler–Natta catalysts, allyltrimethylsilane has so far received little attention. Isotactic poly(allyltrimethylsilane) was first prepared by Natta and coworkers with a $TiCl_4/AlEt_3$ catalyst[1]. For the different fractions obtained from solvent fractionation, they reported viscosity, density and melting points. The more crystalline fraction (insoluble in refluxing xylene) has a very high melting point of 360°C and its X-ray fibre spectrum shows a helix structure with ternary symmetry (identity period 6.5 Å) attributed to an isotactic structure. Amorphous, probably largely atactic fractions, were also obtained with this low-specificity catalyst. Despite the very high melting point and low solubility of the crystalline fraction of isotactic poly(allyltrimethylsilane), no other characterization of this polymer has appeared since.

The discovery of stereospecific metallocene polymerization catalysts allowed the synthesis of both isotactic[2–7] and syndiotactic[8–12] poly(α-olefins), with the latter constituting a new family of polymers. As part of our continuing interest in new polyolefin structures, we explored the synthesis of allyltrimethylsilane polymers (PATMS) with zirconocene/methylalumoxane (MAO) homogeneous catalysts. In this paper we report on a preliminary characterization of atactic (a-PATMS), isotactic (i-PATMS) and syndiotactic (s-PATMS) poly(allyltrimethylsilane) and on the structural characterization of the latter. (s-PATMS prepared with the $Me_2C(Cp)(Flu)ZrCl_2$/MAO catalyst has been reported in the patent literature[13,14]. For a polymer with $[\eta]=0.48$, a T_m of 263°C was found[13].)

EXPERIMENTAL

Allyltrimethylsilane (Fluka, 97%) was purified on a Todd fractional distillation apparatus by collecting the middle fraction, which was subsequently vacuum-transferred from CaH_2 and stored under hydrogen. All polymerizations were carried out in dry nitrogen atmosphere in a Schlenk tube equipped with side arm for nitrogen inlet and magnetic stirring bar, thermostated at the required temperature by an external water bath. MAO (Schering, 30% toluene solution) was vacuum-dried to a white, free-flowing powder. Bis(η^5-indenyl)zirconium dichloride (Ind_2ZrCl_2)[15], *rac*-dimethylsilylbis(1-η^5-indenyl)zirconium dichloride (*rac*-$Me_2SiInd_2ZrCl_2$)[5] and isopropylidene-(η^5-cyclopentadienyl)(9-η^5-fluorenyl)zirconium dichloride ($Me_2C(Cp)(Flu)ZrCl_2$)[8] were synthesized according to known procedures. The metallocene and MAO were precontacted for 5 min in toluene solution and then added

* To either of whom correspondence should be addressed

0032-3861/94/21/4648–08

to the monomer. The polymerizations were quenched with CH_3OH and the polymers thoroughly washed with the same solvent. Sample 1 was dissolved in $CHCl_3$ and filtered. Sample 4 was exhaustively extracted in refluxing pentane.

Calorimetric measurements were obtained by using a Perkin–Elmer DSC-7 thermal analyser calibrated with indium and tin standards. The melting behaviour of the as-polymerized samples was studied with standard cooling and heating rates of $10°C\,min^{-1}$. In some cases, when specified, different heating and cooling rates were used.

Solution ^{13}C n.m.r. spectra were run at 75.4 MHz on a Varian Unity-300 n.m.r. spectrometer. Samples were run as 5% solutions in *o*-dichlorobenzene-d_4 (ODCB, MSD Isotopes) at 130°C. Chemical shifts are referenced to tetramethylsilane (TMS) using as a secondary reference the carbon resonance for the chlorinated carbons of ODCB-d_4 at 132.9 ppm. Some 6000 transients were accumulated for each spectrum with a 10 s delay period between pulses. Gated decoupling was used to inhibit the nuclear Overhauser enhancement. The proton n.m.r. spectra were run on 2.5% solutions on ODCB-d_4 at 299.95 MHz on the same spectrometer. Some 128 transients were accumulated with a pulse delay of 10 s. Solid-state ^{13}C n.m.r. spectra were run at 67.9 MHz on a Chemagnetics CMX-270 n.m.r. spectrometer. The samples were spun at the magic angle at speeds near 5 kHz. Cross-polarization with a 1 ms contact period was used, with r.f. power levels set so that $\gamma(H_2)$ was $4 \times 10^5\,s^{-1}$ for both the ^{13}C and proton channels. Some 500 transients were acquired for each solid-state n.m.r. spectrum. Chemical shifts are reported relative to the methyl resonance of hexamethylbenzene at 16.9 ppm. The n.m.r. data were transferred to a work-station running Varian's VNMR software package for data reduction. In order to determine accurately the peak positions for overlapping resonances, the spectra were deconvoluted using the spectrum deconvolution routine in VNMR. The T_1^C measurements were made using cross-polarization spin excitation as described by Torchia[16].

Wide-angle X-ray diffraction patterns were obtained with nickel-filtered Cu Kα radiation. The diffraction patterns of unoriented samples were obtained with an automatic Philips diffractometer, while those for oriented samples were obtained with a photographic cylindrical camera.

The evaluation of the degree of crystallinity for the different s-PATMS specimens was performed on completely unoriented samples, as verified by photographic X-ray diffraction patterns. Since compression-moulding procedures generate some crystalline orientation also for low pressures, unoriented melt-crystallized samples were obtained by heating the specimens in a N_2 atmosphere at 330°C and then quenching to room temperature.

RESULTS AND DISCUSSION

Since the relationship between the metallocene symmetry and the consequent polymer structure was consistently obeyed for a number of 1-olefins from propylene[2,8,9] up to 4-methyl-1-pentene[7,10,11] and 4-methyl-1-hexene[10,12], it was expected that similar relationships would be observed for the polymerization of allyltrimethylsilane. It was therefore expected that a-PATMS would be obtained from achiral metallocenes with a higher C_{2v} symmetry such as bis(η^5-cyclopentadienyl)zirconium dichloride (Cp_2ZrCl_2), bis(η^5-pentamethylcyclopentadienyl)zirconium dichloride ($Cp^*_2ZrCl_2$) or bis(η^5-indenyl)zirconium dichloride (Ind_2ZrCl_2). i-PATMS was the expected product from C_2-symmetric metallocenes such as *rac*-ethylene-bis(1-η^5-indenyl)zirconium dichloride (*rac*-EBIZrCl$_2$) or *rac*-dimethylsilylbis(1-η^5-indenyl)zirconium dichloride (*rac*-$Me_2SiInd_2ZrCl_2$); and s-PATMS was expected from C_s-symmetric metallocenes such as isopropylidene-(η^5-cyclopentadienyl)(9-η^5-fluorenyl)zirconium dichloride ($Me_2C(Cp)(Flu)ZrCl_2$). Although both Cp_2ZrCl_2/MAO and $Cp^*_2ZrCl_2$/MAO catalysts gave only allyltrimethylsilane dimers and low oligomers with no tacticity information[17], Ind_2ZrCl_2/MAO produced an amorphous, solid polymer (sample 1), while both *rac*-$Me_2SiInd_2ZrCl_2$/MAO (samples 2 and 3) and $Me_2C(Cp)(Flu)ZrCl_2$/MAO (samples 4 and 5) produced crystalline, high-melting materials. Selected polymerization results are reported in *Table 1*.

An i-PATMS (sample 6) obtained from $TiCl_4/AlEt_3$† provided us with reference X-ray, i.r. and solid-state n.m.r. spectra for isotactic poly(allyltrimethylsilane), thus confirming an isotactic structure and s(3/1) helix conformation for sample 2. Viscosities and standard d.s.c. analysis for samples 1–5 are reported in *Table 2*. The amorphous, low-molecular-weight sample 1 is fully soluble in $CHCl_3$ at room temperature as well as in ODCB and tetrahydronaphthalene (THN) at 135°C. Sample 2 becomes soluble

† 20 ml of ATMS were polymerized at 85°C for 8 h with a preformed $TiCl_4$ (0.25 ml)/$AlEt_3$ (0.63 ml) catalyst according to ref. 1, yielding 5.54 g of polymer. After washing with CH_3OH/HCl and CH_3OH, the polymer was fractionated by exhaustive Kumagawa extraction with solvents of increasing boiling points: acetone (46%, oil); diethyl ether (18%, amorphous solid); n-heptane (2%, $T_m = 118.5$°C, $\Delta H_f = 9.2\,J\,g^{-1}$). The insoluble fraction (34%, $T_m = 305.4$°C (major), 291.3°C (minor), $\Delta H_f = 35.6\,J\,g^{-1}$) had i.r., s.s. n.m.r. and X-ray powder diffraction (crystallinity 40%) spectra identical to those of i-PATMS sample 2

Table 1 Allyltrimethylsilane polymerization with metallocene/MAO catalysts

Sample	Metallocene	Amount (μmol)	Al[a] (mmol)	T_p (°C)	t_p (h)	ATMS (ml)	Yield (g)
1	Ind_2ZrCl_2	8.98	8.7	22	22	20	10.53
2	*rac*-$Me_2SiInd_2ZrCl_2$	4.46	5.1	50	2	10	6.93
3	*rac*-$Me_2SiInd_2ZrCl_2$	2.23	2.2[b]	80	2	20	13.16
4	$Me_2C(Cp)(Flu)ZrCl_2$	9.25	8.8	20	24	43	23.67
5	$Me_2C(Cp)(Flu)ZrCl_2$	9.16	8.51	50	4	50	19.88

[a] MAO, isolated powder
[b] MAO, 30% toluene solution

Table 2 Characterization of PATMS samples[a]

Sample	Tacticity	$[\eta]$ (dl g^{-1})	P_n[b]	T_m (°C)	ΔH_f (J g^{-1})	T_c (°C)	ΔH_c (J g^{-1})	T_g (°C)
1	Atactic[c]	0.08	51			Amorphous		24
2	Isotactic[d]	ins.		*e*	28	*f*	−34	
3	Isotactic[c]		41	*g*	42	267	−43	
4	Syndiotactic	1.75		283	23	234	−23	
5	Syndiotactic[c]	0.90		259	16	230	−19	42

[a] Intrinsic viscosities measured in THN at 135°C; d.s.c. measurements with standard heating and cooling rates of 10°C min^{-1}; the melting transitions of the second fusion are reported
[b] Approximate number-average polymerization degree, from unsaturated end-groups, ^{1}H n.m.r.
[c] From ^{1}H n.m.r.
[d] By comparison with an authentic sample of i-PATMS, see ref. 17
[e] Three peaks: 269°C (0.3 J g^{-1}), 283.5°C (7.9 J g^{-1}), 295.1°C (20 J g^{-1})
[f] Two peaks: 252.9°C, 267.0°C
[g] Three peaks: 257.4°C, 282°C, 288.9°C

Table 3 Solution ^{13}C n.m.r. chemical shifts[a] of PATMS samples 1, 3 and 5

Assignment	Sample 1 a-PATMS	Sample 3 i-PATMS	Sample 5 s-PATMS
CH_2 backbone	45.6–47.8	46.7_5	46.9_9
CH backbone	29.3–31.3	29.7_1	29.5_5
CH_2–Si	23.2–24.9	23.9_5	24.0_4
–Si–CH_3	−0.4–1.1	0.4_0	0.1_9

[a] δ (ppm), referenced to TMS

in both THN and ODCB only at 180°C, but reprecipitates upon cooling at 135°C. The lower-molecular-weight sample 3 is partially soluble in $CHCl_3$ and fully in ODCB. The just polymerized sample 4 was soluble in all solvents, but upon standing (ca. 1 month) it became completely insoluble in $CHCl_3$ and could be dissolved only after prolonged heating at 180°C in THN, in which it then remained soluble at 135°C. Its lower-molecular-weight counterpart, sample 5, is soluble in warm ODCB.

Solution n.m.r. analysis

Given their very low solubility, no solution n.m.r. analysis could be carried out on samples 2 and 4. However, ^{1}H n.m.r. analysis of the soluble samples 1, 3 and 5 enabled us to assign their tacticities and, by inference, those of the insoluble samples 2 and 4. All resonances in the proton n.m.r. spectrum of sample 1 are broad, except the one at 0.1 ppm ($SiMe_3$ protons). An unresolved resonance at 1.0–1.5 ppm indicates an atactic structure. Olefinic protons are detectable at 4.60 and 4.65 ppm, and are consistent with a vinylidene end-group structure arising from β-hydrogen elimination; the number-average polymerization degree (P_n) calculated from the chain methylene/olefinic protons peak areas (thus neglecting possible chain transfer to aluminium) gives a value of 51. The ^{1}H n.m.r. spectrum of the $CHCl_3$ soluble portion of sample 3 is diagnostic of an isotactic microstructure: the resonance of the chain methylene protons is split into two peaks at 1.1 and 1.2 ppm as expected for two diastereotopic methylene protons in a *meso* dyad. The olefinic resonances at 4.59 and 4.63 ppm are again consistent with a vinylidene end-group structure arising from β-H elimination; chain methylene/olefinic protons peak areas give a P_n of 41. Finally, the ^{1}H n.m.r. spectrum of samples 5 shows a single resonance at 1.0–1.2 ppm, diagnostic of a syndiotactic structure (two equivalent chain methylene protons).

The ^{13}C n.m.r. peak assignments in *Table 3* were made using chemical shift additivity rules and attached proton test (APT) data. Several smaller peaks present in the spectra of samples 1 and 3 were not assigned but, given their low molecular weight, are likely to be due to end-groups. Sample 1 shows only broad, unresolved resonances. The broadest peak (thus the more sensitive to the stereochemical environment) appears to be the chain methylene carbon at 45.6–47.8 ppm. This confirms the atacticity of sample 1 and the complete aspecificity of the Ind_2ZrCl_2 metallocene, previously observed for propene and 1-butene polymerization[18].

Samples 3 and 5 show only minor differences in their ^{13}C n.m.r. spectra as a result of polymer tacticity, but the narrow width of the four resonances is indicative of high stereoregularity. As can be seen from *Table 3*, the observed shift differences between the two samples are 0.2 ppm or less, but the directions of the shifts are consistent with those observed for other polyolefins[19]. While the observed chemical shifts in PATMS as a function of polymer tacticity are large enough to evaluate whether a sample is primarily isotactic or syndiotactic, it is difficult to quantitate even the dyad populations in the polymers with any confidence. However, from the combined proton and carbon n.m.r. data we can safely assign an atactic structure to sample 1, confirm the isotactic structure of sample 3 (hence of sample 2) and assign the syndiotactic structure to sample 5 (hence to sample 4); thus the metallocene symmetry–polymer tacticity relationship is still obeyed with the very bulky allyltrimethylsilane monomer. These assignments are in agreement with those from solid-state n.m.r. (see below).

Thermal analysis and X-ray diffraction

The d.s.c. endotherms of i-PATMS crystallized from the melt show at least two peaks. The peak areas are dependent on the thermal history of the samples. In order to examine the dependence of the ratio of the areas on the heating and cooling rates, i-PATMS sample 2 was studied with the following d.s.c. conditions: heating rates of 2.5, 5, 10 and 20°C min^{-1} after cooling from the melt at 5°C min^{-1}, and constant heating rate of 5°C min^{-1} after cooling from the melt at different cooling rates of 40, 10, 2 and 0.5°C min^{-1}. The ratio of the two areas of the melting peaks of sample 2 is dependent on the cooling

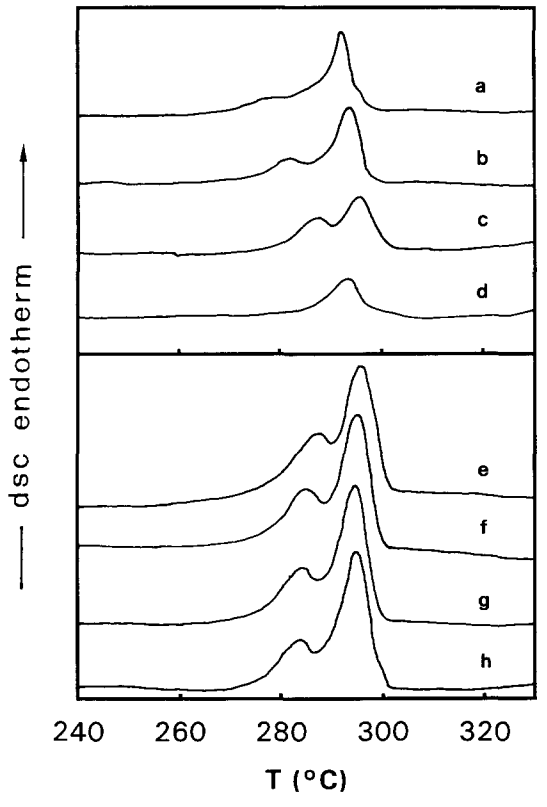

Figure 1 D.s.c. traces of the fusion (5°C min^{-1}) of i-PATMS sample 2 after melting at 330°C for 5 min and cooling at different rates: (a) 40°C min^{-1}; (b) 10°C min^{-1}; (c) 2°C min^{-1}; (d) 0.5°C min^{-1}. D.s.c. traces of the fusion at different rates after cooling at 5°C min^{-1}: (e) 20°C min^{-1}; (f) 10°C min^{-1}; (g) 5°C min^{-1}; (h) 2.5°C min^{-1}

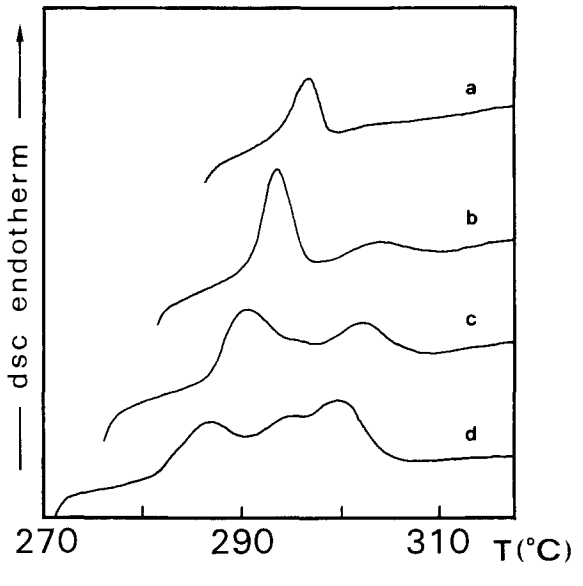

Figure 2 D.s.c. traces of the fusion (10°C min^{-1}) of i-PATMS sample 2 after isothermal crystallization (60 min) at different temperatures: (a) $T_c = 285$°C; (b) $T_c = 280$°C; (c) $T_c = 275$°C; (d) $T_c = 270$°C

rate during crystallization (*Figures 1a–d*) but scarcely on the heating rate (*Figures 1e–h*). A complex melting behaviour is shown also by the d.s.c. traces of i-PATMS isothermally crystallized from the melt at different temperatures (*Figure 2*).

Despite this complex melting behaviour, no phenomenon of polymorphism has been oserved for i-PATMS. In fact, for instance, the X-ray diffraction patterns of sample 2 cooled from the melt at 10°C min^{-1} (*Figure 1b*) or 0.5°C min^{-1} (*Figure 1d*) are identical (*Figure 3*). This suggests that the phenomena pointed out by the d.s.c. analysis involve only some morphological reorganization of the crystalline phase.

The X-ray diffraction patterns of three different specimens of one s-PATMS polymer (sample 4), as polymerized, annealed at 260°C for 20 min and melt crystallized, are shown in *Figures 4a*, *4b* and *4c*, respectively. X-ray diffraction patterns analogous to that of *Figure 4a* are obtained for samples cast from solutions

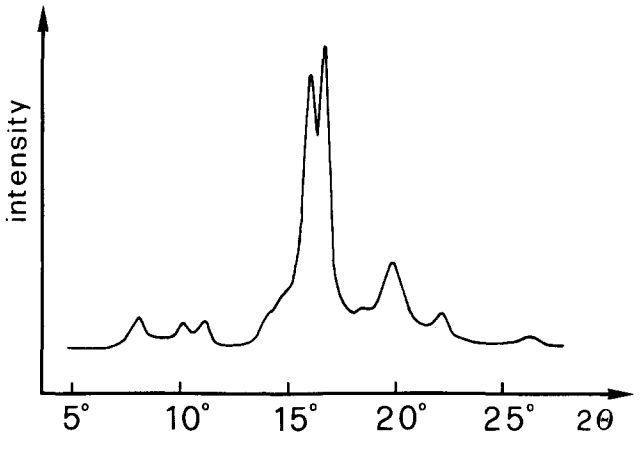

Figure 3 X-ray diffraction pattern of i-PATMS sample 2 after cooling from the melt at 0.5°C min^{-1}, corresponding to the d.s.c. trace reported in *Figure 1d*

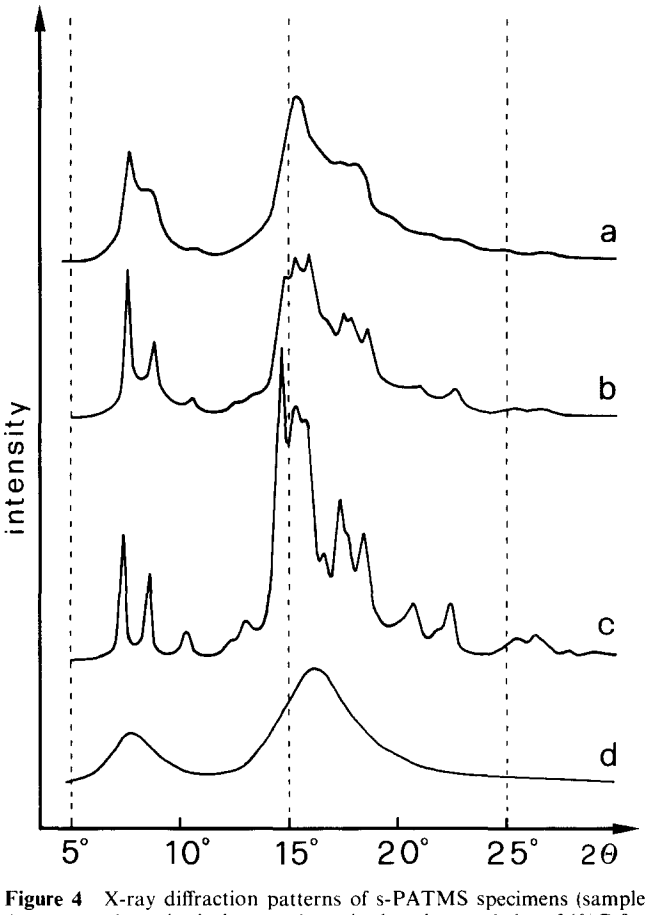

Figure 4 X-ray diffraction patterns of s-PATMS specimens (sample 4): (a) as-polymerized; (b) as-polymerized and annealed at 260°C for 20 min; (c) melt-crystallized. The X-ray diffraction pattern of the a-PATMS sample 1 is reported in (d)

Table 4 Comparison between the diffraction angles, 2θ, of the reflections in the X-ray patterns of oriented and unoriented s-PATMS (sample 4)[a]

Unoriented samples, 2θ (deg)		Oriented sample		
As prepared	Compression moulded	2θ (deg)	Intensity	Layer
7.6	7.3	7.3	m	0
8.6(b)	8.5	8.5	mw	0
10.8(b)	10.3	10.3	w	0
	12.3(sh)	12.4	vw	0
	13.0	12.9	vw	1
	14.6			
		14.8(b)	vs	1
15.4(b)	15.2			
	15.8	15.7	s	1
	16.4	16.3	w	0
17.4(b)	17.3	17.4	m	0
	17.6(sh)	17.5	vvw	1
18.0(b)	18.4	18.4	m	0
	20.7	20.7	w	0
21.5(b)	21.8(sh)			
22.5(b)	22.3	22.4	m	0
	25.4(b)			
	26.2	26.0	vw	2

[a] b = broad diffraction, sh = shoulder; vs = very strong, s = strong, m = medium, mw = medium weak, w = weak, vw = very weak, vvw = very very weak

of s-PATMS in different solvents (e.g. heptane or chloroform). Attempts to quench this polymer to the amorphous state for an evaluation of the amorphous contribution to the diffraction patterns of these samples were unsuccessful, so the shape of the diffraction halo of the atactic PATMS (sample 1), shown in *Figure 4d*, was used. The pattern of *Figure 4a* presents mainly broad peaks, at the diffraction angles indicated in column 1 of *Table 4*, superimposed on two intense amorphous diffraction halos. The patterns of *Figures 4b* and *4c* present, instead, several well defined narrow diffraction peaks (more clearly apparent in *Figure 4c*), whose 2θ positions are listed in column 2 of *Table 4*, superimposed on smaller amorphous diffraction halos. The degrees of crystallinities, as evaluated by the X-ray diffraction data of *Figures 4a, 4b* and *4c*, are roughly equal to 30%, 40% and 60%, respectively. The information of the X-ray diffraction fibre pattern (the 2θ positions, the relative intensities of the observed reflections and the layer line indexes l) of an oriented melt-spun sample is also reported in *Table 4* (columns 3–5). The fibre pattern of s-PATMS shows the presence of two different layer lines, besides the equatorial layer line, whose ζ reciprocal coordinates are consistent with l indexes 1 and 2 for repeat unit $c = 7.1 \pm 0.3$ Å.

These data are consistent with a helical symmetry of the kind s(2/1)2, in which the chain repetition occurs after two conformational repeating units[20] (four monomeric units) and after one turn around the chain axis. This kind of symmetry has also been observed in polymorphic forms of several syndiotactic vinyl polymers: polypropene[21], polystyrene[22–24], poly(*p*-methylstyrene)[25] and polybutene[26]. By a comparison between the data of *Table 4*, it is apparent that all the broad peaks of the as-polymerized sample nearly correspond to the main diffraction peaks of the melt-crystallized (unoriented and oriented) samples. It seems reasonable to conclude that all the considered specimens of s-PATMS sample 4 are in a same crystalline form, and that the differences between the observed diffraction patterns are substantially due to different degrees of crystallinity (which make the amorphous halo more prominent for the pattern of *Figure 4a*) and different sizes of the crystallites (smaller for the as-polymerized specimen of *Figure 4a*, corresponding to broader reflections).

A closer comparison between the X-ray diffraction patterns of unoriented samples of *Figure 4* shows that the strong Bragg reflections of the first layer line (located at 14.6°, 15.2° and 15.8° in the patterns of *Figures 4b* and *4c*, see also *Table 4*) are substituted, for the more poorly crystallized sample, by a broad peak centred at 15.4°. In particular, the very strong peak at 14.6° (*Figure 4c*) is not present even as a shoulder (*Figure 4a*). On the contrary, weaker equatorial reflections, like those at 8.5°, 10.3°, 17.3° and 18.4°, although becoming broader, remain detectable also in the patterns of *Figure 4a*. This should correspond to the presence in the crystalline form, for the specimen of *Figure 4a*, of some kind of structural disorder. In particular, the more rapid disappearance of the Bragg reflections of the non-equatorial layer lines suggests the introduction of rotational (about the chain axis) and/or translational (along the axis) disorder between the packed chains, which roughly preserve the chain conformation and the periodic placements of the axis of the chain molecules[27,28].

A more complete characterization of the packing disorder in these poorly crystallized samples (as-polymerized and cast from solutions) could be obtained by X-ray diffraction patterns of oriented samples. Unfortunately, all our attempts to get orientation in cast films by drawing were unsuccessful, owing to brittleness of the samples.

The d.s.c. scans of the three different specimens of sample 4 of *Figures 4a* (as-polymerized), *4b* (annealed at 260°C) and *4c* (melt-crystallized) are shown in *Figures 5a*, *5b* and *5c*, respectively. The endothermic melting peaks are located at 272, 280 and 283°C and the melting enthalpy is of nearly 14, 15 and 28 J g^{-1}, respectively. The melting enthalpy data confirm a degree of crystallinity for the melt-crystallized sample much higher than

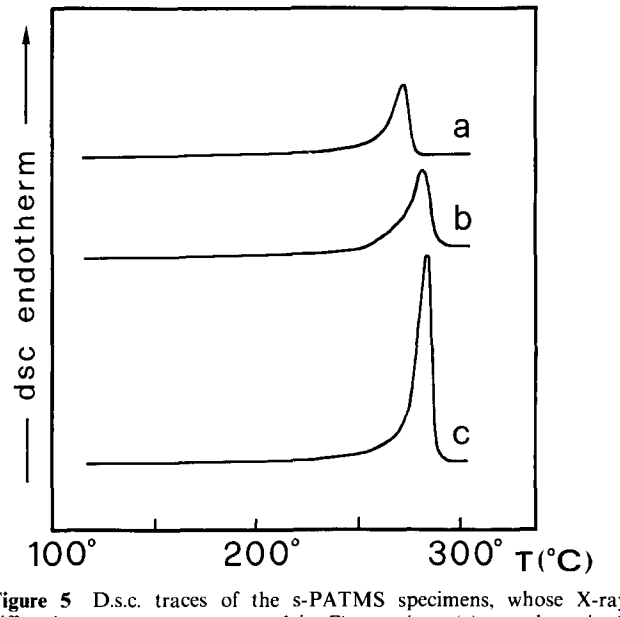

Figure 5 D.s.c. traces of the s-PATMS specimens, whose X-ray diffraction patterns are reported in *Figures 4a–c*: (a) as-polymerized; (b) as-polymerized and annealed at 260°C for 20 min; (c) melt-crystallized

for the as-polymerized and annealed samples. The similar melting enthalpies of the as-prepared and annealed samples (which according to the X-ray diffraction patterns should have markedly different crystallinities) are, of course, due to the annealing that occurs during the scan[29].

Solid-state n.m.r.

Samples 1–5 as-prepared and sample 4 after melt crystallization were studied by ^{13}C c.p.-m.a.s. n.m.r. spectroscopy. The c.p.-m.a.s. (cross-polarization magic-angle spinning) spectra were assigned by analogy to the solution-state n.m.r. assignments and are presented in *Table 5*. The spectra of a-PATMS (sample 1) and of i-PATMS (sample 2) are shown in *Figure 6*, while those of s-PATMS sample 4 as-polymerized and after melt crystallization are shown in *Figure 7*. a-PATMS exhibits broad resonances encompassing the entire range of resonance positions observed for the isotactic and syndiotactic polymers. This range of resonance frequencies is consistent with the disorder expected in an atactic polymer. The major resonances in the spectra of i-PATMS samples 2 and 3 are narrow, consistent with local conformational order due to the regular tacticity of the polymer. The position of the CH_2 backbone resonance near 45 ppm is between the positions of the two backbone methylene resonances observed in s-PATMS (see below). Since the resonance frequency of the chain methylene is primarily a function of the local conformations of the polymer chain[30], it appears that in i-PATMS one of the carbons that is γ to the CH_2 is in a *gauche* conformation and the other γ carbon is in a *trans* conformation. This occurrence of alternating *gauche–trans* conformations is similar to that observed for isotactic polypropene, which crystallizes in a s(3/1) helical conformation[31]. This assignment is totally consistent with the X-ray data. Relatively broad resonances were observed as shoulders on the downfield sides of the CH_2 and CH backbone resonances in the i-PATMS samples. Given the broadness of these peaks and the previous observation of a similar CH_2 shoulder due to the non-crystalline component of isotactic polypropene[32], the downfield shoulders were assigned to non-crystalline components of the samples. The chemical shift observed for the shoulder of the backbone methylene resonance is near 46.3 ppm.

The solid-state ^{13}C n.m.r. spectrum of highly crystalline melt-crystallized s-PATMS, shown in *Figure 7a*, shows two distinct resonances representing the chain methylene carbons. The separation of 7 ppm between these resonances is similar to those observed for the crystalline forms

Table 5 Solid-state ^{13}C n.m.r. chemical shifts of PATMS samples 1, 2, 4 as-polymerized and sample 4 melt-crystallized

Sample	Carbon	δ(ppm)	Comment[a]
1	CH_2 backbone	49–42	
a-PATMS	CH backbone	29.6–28.1	
	$-CH_2-Si$	25–22	
	$-Si-CH_3$	0.6	
2	CH_2 backbone	44.8	*trans–gauche*
i-PATMS	CH backbone	27.3	
	$-CH_2-Si$	21.9–21.2	
	$-Si-CH_3$	1.2	
4	CH_2 backbone	46.9	*trans–trans*
s-PATMS		44.3–43.4	*gauche–trans*
as-polymerized		40.5	*gauche–gauche*
	CH backbone	29.5	amorphous
		28.0	crystalline
		27.2	crystalline
	$-CH_2-Si$	24.4	amorphous
		21.6	crystalline
		20.7	crystalline
	$-Si-CH_3$	1.0	crystalline
		0.2	crystalline
4	CH_2 backbone	47.1	*trans–trans*
s-PATMS		40.5	*gaughe–gauche*
melt-crystallized	CH backbone	29.0	amorphous
		27.5	crystalline
		26.8	crystalline
	$-CH_2-Si$	20.7	crystalline
	$-Si-CH_3$	0.2	crystalline

[a] See text

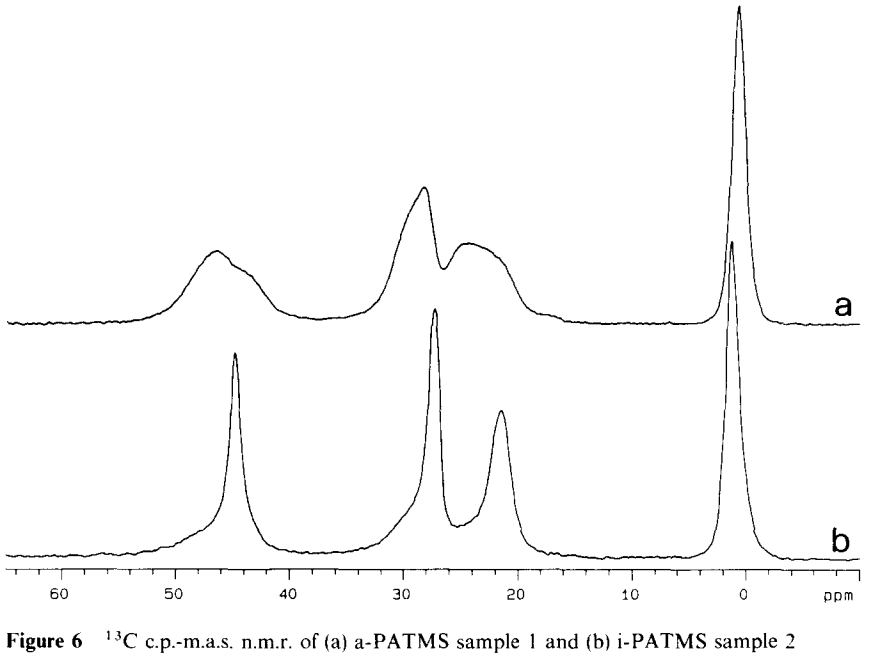

Figure 6 ^{13}C c.p.-m.a.s. n.m.r. of (a) a-PATMS sample 1 and (b) i-PATMS sample 2

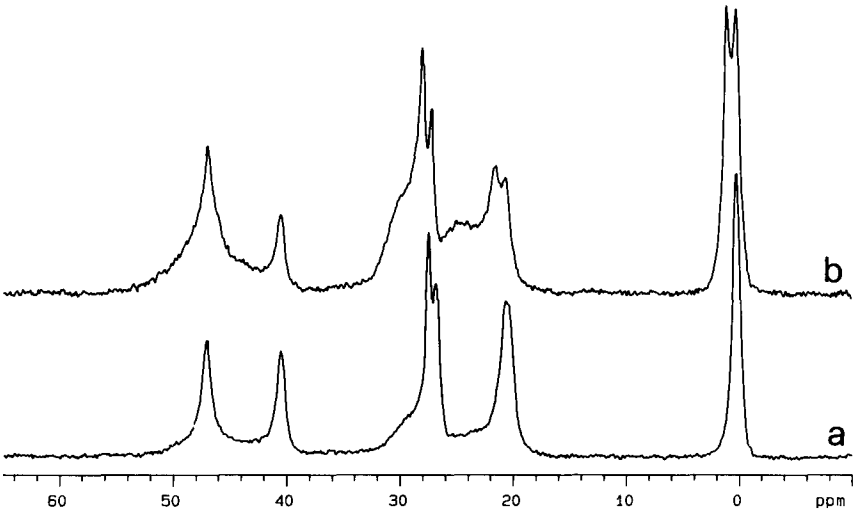

Figure 7 ^{13}C c.p.-m.a.s. n.m.r. of (a) s-PATMS sample 4 after melt crystallization and (b) s-PATMS sample 4 as-polymerized

Table 6 Solid-state ^{13}C spin–lattice relaxation time (T_1^C) for s-PATMS sample 4 as-polymerized

δ (ppm)[a]	Assignment	T_1^C (s)[b]
46.9	CH_2 crystalline	37±6
44.3 to 43.4	CH_2 non-crystalline	9±2
40.5	CH_2 crystalline	77±13
29.5	CH non-crystalline	13±1
28.0	CH crystalline	57±7
27.2	CH crystalline	120±20
24.4	pendent CH_2 non-crystalline	6±1
21.6	pendent CH_2 crystalline	30±5
20.7	pendent CH_2 crystalline	24±4
1.0	CH_3–Si	1.5±0.3
0.2	CH_3–Si crystalline	2.1±0.3

[a] Chemical shift
[b] T_1^C ± standard deviation of the T_1^C value

with chains in the helical s(2/1)2 conformation of syndiotactic polypropene[33], syndiotactic polystyrene[34] and syndiotactic poly(*p*-methylstyrene)[35]. This pairing of the chain methylene resonances suggests that s-PATMS has a helical structure in the crystalline phase, corresponding to *trans–trans–gauche–gauche* sequences of dihedral angles. In this case the CH_2 resonances at 47.1 and 40.5 ppm represent the two crystallographically distinct methylene carbons that have γ carbons in *trans–trans* and *gauche–gauche* conformations, respectively. This agrees well with the s(2/1)2 helical symmetry indicated by the X-ray diffraction data of the previous section.

Three backbone CH resonances are observed at 29.0, 27.5 and 26.8 ppm. The resonance at 29.0 ppm is relatively broad and is probably due to non-crystalline polymer. Since the melt-crystallized sample 4 is highly crystalline and the X-ray diffraction data show a consequent high degree of order in the crystalline phase, it is possible that the two resonances at 27.5 and 26.8 ppm can be associated with some inequivalence of the carbons in the unit cell, as observed, for instance, in the solid-state n.m.r. spectra of isotactic polypropylene in the α-crystalline form[31].

The ^{13}C c.p.-m.a.s. n.m.r. spectrum of sample 4, s-PATMS as polymerized, is shown in *Figure 7b*. As shown in the X-ray diffraction section of this paper, sample 4 as-polymerized is less crystalline than the melt-crystallized. This is consistent with the presence of the broad resonances at 29.5 and 24.4 ppm possibly associated with the amorphous phase. The appearance of a broad CH_2 main-chain resonance near 47 ppm shows that the backbone bonds of the chains in the non-crystalline s-PATMS phase exhibit a large percentage of *trans* conformations.

Two new resonances appear at 1.0 and 21.6 ppm and, contrary to the other resonances whose positions are not altered, the CH resonances at 26.8 and 27.5 ppm appear to be shifted to 27.2 and 28.0 ppm.

To characterize better the nature of the multiple resonances in s-PATMS, the solid-state n.m.r. T_1^C values for sample 4, as-polymerized, were determined and can be found in *Table 6*. Assuming T_1^C is predominantly via a dipole–dipole relaxation mechanism[36], the value of T_1^C is an indicator of local molecular motion. In the case of a solid polymer at a sample temperature above the glass transition temperature, a short value of T_1^C usually indicates greater mobility and can therefore be associated with non-crystalline components of the polymer. An exception to this rule-of-thumb are methyl groups, which usually have short T_1^C values due to rapid rotation. The results in *Table 6* show that those carbons associated with crystalline components of the s-PATMS have T_1^C values ranging from about 24 s for the pendent CH_2 resonances to greater than 100 s for the backbone CH resonance. Those carbons representing the non-crystalline components of the polymer exhibit T_1^C values that are about 5 times smaller than those for the analogous crystalline carbons. Based on these observations, the T_1^C data in *Table 6* show that the pendent CH_2 resonances at 21.6 and 20.7 ppm and both of the CH resonances at 28.0 and 27.2 ppm represent rigid, and therefore crystalline, components of the s-PATMS.

Additional remarks on s-PATMS structure

A major question arising from this study is the nature of the additional CH_3 and CH_2 side-chain resonances in the solid-state n.m.r. spectra of the as-prepared s-PATMS sample. Also the observed shifts of the two CH resonances could be interpreted as due to the disappearance of the splitting typical of the melt-crystallized samples (resonances at 27.5 and 26.8 ppm, merging into a single

resonance at 27.2 ppm, as generally occurs when not well crystallized samples are considered[30,31]) and the appearance of a new resonance at 28.0 ppm, which would have the same origin as the two new resonances of *Figure 7b* (at 1.0 and 21.6 ppm).

A reasonable hypothesis is that these additional resonances could be related to an additional interchain facing possibly related to the unknown packing disorder suggested by the X-ray diffraction characterization.

In a recent paper relative to a solid-state n.m.r. characterization of syndiotactic polypropene[37], it has been suggested that a nearly 1:1 CH_3 splitting, observed for annealed samples, would be due to statistical replacements of chains of opposite chirality within a lattice with a regular disposition of the chains. In our opinion an analogous kind of packing disorder could be present in the poorly crystallized samples of s-PATMS.

ACKNOWLEDGEMENTS

We thank Dr F. Piemontesi for the synthesis of the metallocenes, R. Mazzocchi and G. Franciscono for the polymerizations, and Pat Faline, who ran the n.m.r. spectra. This work was supported by the Ministero dell'Università e delle Ricerce Scientifice e Technologice, and by the Progetto Finelitteto Chimica Fine e Secondria of the CNR.

REFERENCES

1 Natta, G., Mazzanti, G., Longi, P. and Bernardini, F. *J. Polym. Sci.* 1958, **31**, 181
2 Ewen, J. *J. Am. Chem. Soc.* 1984, **106**, 6355
3 Kaminsky, W., Külper, K., Brintzinger, H. H. and Wild, F. *Angew. Chem. Int. Edn Engl.* 1985, **24**, 507
4 Ewen, J., Haspeslagh, L., Atwood, J. and Zhang, H. *J. Am. Chem. Soc.* 1987, **109**, 6544
5 Herrmann, W., Rohrmann, J., Herdtweck, E., Spaleck, W. and Winter, A. *Angew. Chem. Int. Edn Engl.* 1989, **28**, 1511
6 Röll, W., Brintzinger, H. H., Rieger, B. and Zolk, R. *Angew. Chem. Int. Edn Engl.* 1990, **29**, 279
7 Kioka, M., Tsutsui, T., Ueda, T. and Kashiwa, N. in 'Catalytic Olefin Polymerization' (Eds T. Keii and K. Soga), Stud. Surf. Sci. Catal., Vol. 56, Elsevier, Amsterdam, 1990, p. 483
8 Ewen, J., Jones, R., Razavi, A. and Ferrara, J. *J. Am. Chem. Soc.* 1988, **110**, 6255
9 Ewen, J., Elder, M., Jones, R., Curtis, S. and Cheng, H. in 'Catalytic Olefin Polymerization' (Eds T. Keii and K. Soga), Stud. Surf. Sci. Catal., Vol. 56, Elsevier, Amsterdam, 1990, p. 439
10 Albizzati, E., Resconi, L. and Zambelli, A. Eur. Pat. Appl. 387609 to Himont, 1990
11 Asanuma, T., Nishimori, Y., Ito, M., Uchikawa, N. and Shiomura, T. *Polym. Bull.* 1991, **25**, 567
12 Zambelli, A., Grassi, A., Galimberti, M. and Perego, G. *Makromol. Chem., Rapid Commun.* 1992, **13**, 269
13 Asanuma, T., Kawanishi, K., Matsuzawa, H. and Nishimori, Y. Eur. Pat. Appl. 438710 to Mitsui Toatsu, 1991
14 Resconi, L., Albizzati, E., Piemontesi, F. and Franciscono, G. It. Pat. IT 131/MI91A to Himont, 1991
15 Samuel, E. and Setton, R. *J. Organomet. Chem.* 1965, **4**, 156
16 Torchia, D. *J. Magn. Reson.* 1978, **30**, 613
17 Resconi, L., Piemontesi, F., Franciscono, G., Abis, L. and Fiorani, T. *J. Am. Chem. Soc.* 1992, **114**, 1025
18 Resconi, L., Abis, L. and Franciscono, G. *Macromolecules* 1992, **25**, 6814
19 Asakura, T., Demura, M. and Nishiyama, Y. *Macromolecules* 1991, **24**, 2334
20 IUPAC Commission on Macromolecular Nomenclature, *Pure Appl. Chem.* 1981, **53**, 733
21 Corradini, P., Natta, G., Ganis, P. and Temussi, P. A. *J. Polym. Sci. (C)* 1967, **16**, 2477
22 Corradini, P., Napolitano, R. and Pirozzi, B. *Eur. Polym. J.* 1990, **26**, 157
23 Immirzi, A., De Candia, F., Iannelli, P., Vittoria, V. and Zambelli, A. *Makromol. Chem., Rapid Commun.* 1988, **9**, 761
24 Guerra, G., Vitagliano, V. M., De Rosa, C., Petraccone, V. and Corradini, P. *Macromolecules* 1990, **23**, 1539
25 Iuliano, M., Guerra, G., Petraccone, V., Corradini, P. and Pellecchia, C. *New Polym. Mater.* 1992, **3**, 133
26 De Rosa, C., Venditto, V., Guerra, G., Pirozzi, B. and Corradini, P. *Macromolecules* 1991, **24**, 5645
27 Corradini, P. and Guerra, G. *Adv. Polym. Sci.* 1992, **100**, 183
28 Clark, E. S. and Muus, L. T. *Z. Kristallogr.* 1962, **117**, 108
29 Wunderlich, B. in 'Macromolecular Physics', Vol. 3, Academic Press, New York, 1980, Ch. IX
30 Tonelli, A. E. in 'NMR Spectroscopy and Polymer Microstructure', VCH, New York, 1989
31 Bunn, A., Cudby, M. E. A., Harris, R. K., Packer, K. J. and Say, B. T. *Polymer* 1982, **23**, 694
32 Kitamaru, R., Horii, F., Nakagawa, M., Saito, S. and Moteki, Y. *Koenshu-Kyoto Daigaku Sen'i Kenkyusho* 1988, **45**, 1
33 Bunn, A., Cudby, M. E. A., Harris, R. K., Packer, K. J. and Say, B. T. *J. Chem. Soc., Chem. Commun.* 1981, 15
34 Grassi, A., Longo, P. and Guerra, G. *Makromol. Chem., Rapid Commun.* 1989, **10**, 687
35 Guerra, G., Grassi, A., Rice, D. M., Karasz, F. E. and MacKnight, W. J. *Polym. Commun.* 1991, **32**, 430
36 Lyerla, J. R. and Levy, G. C. *Topics C-13 NMR Spectrosc.* 1974, **1**, 79
37 Sozzani, P., Simonutti, R. and Galimberti, M. *Macromolecules* 1993, **26**, 5782